

Laser induced multi-scale textured zirconia coating on Ti-6Al-4V

Anil Kurella · Narendra B. Dahotre

Received: 3 April 2005 / Accepted: 9 August 2005
© Springer Science + Business Media, LLC 2006

Abstract A textured coating of zirconia on Ti-6Al-4V alloy was produced using pulsed laser based processing technique. Scanning electron microscope observations coupled with fractal analysis revealed the multi-scale nature of the textured coating. Both stylus based profilometric measurements and fractal analysis indicated non-linear nature of the relationship between laser processing speed at constant pulse frequency (10 kHz) and roughness of the textured coating. The textured coatings produced with all the three processing speeds (40, 160, 290 cm/min) were fractal over certain length scales. Processing at 40 cm/min resulted in structures that are fractal across a large number of length scales where as higher processing speeds resulted in fractality over fewer length scales. The processing speed influenced the zirconia content in the coating and the phase transformation within Ti-matrix of the coating. Within the coating, while zirconia content decreased the amount of retained β -Ti increased with increase in processing speed. Such physical and chemical transformations are desired in a titanium bio-implant for effective contact with protein, cells and tissues at various length scales and its effective chemical performance in bio-environment.

1. Introduction

Ti and its alloys are excellent biomaterials because of their good biocompatibility and corrosion resistance. The spontaneous formation of a passive TiO₂ layer provides the necessary inertness and biocompatibility [1]. However this TiO₂ layer has inferior mechanical properties and fractures easily under wearing conditions. This results in detrimental accumulation of wear debris and eventual ion release into biosystems [2]. To overcome this problem and to provide effective osseointegration hard and wear resistant bioceramic materials are coated on implant surfaces. Bioceramics like zirconia have good fracture toughness, bending strength apart from excellent biocompatibility and have been coated on Titanium alloys [3, 4].

The other surface engineering processing for implant surfaces involves texturing the surfaces to make the tissues grow into the surface and hold them better. Physical texturing is now recognized to play a major role in the way cells respond to surfaces and thus great deal of studies were dedicated to correlate the proliferation, adhesion, migration and differentiation [5, 6]. Surfaces textured with micro and nano features have been to some extent successful in osseointegration [5, 6]. At this point it is worth remembering that in nature materials are organized at various length scales ranging from nano to micro level. Thus a synthetic material designed to survive and effectively integrate into a bio environment might be expected to show compatibility at multi-scales rather than at a single level. Hence the present emphasis is to develop materials that are functionally active and hierarchically organized at various length scales. So far the efforts to produce integrated micro to nano features for bio applications are limited and rare [5]. There exist many techniques to provide either efficient coatings or textures but so far there has been

A. Kurella · N. B. Dahotre
Department of Materials Science and Engineering,
The University of Tennessee, Knoxville, Tennessee 373996, USA

N. B. Dahotre (✉)
Department of Materials Science and Engineering,
The University of Tennessee, Knoxville, Tennessee 373996, USA;
Materials Processing Group, Metals and Ceramics Division,
Oak Ridge National Laboratory, Oak Ridge, Tennessee 37831,
USA
Tel.: 865-974-3609
e-mail: ndahotre@utk.edu

no effort to effectively integrate both coatings and texture together to produce textured coatings [6].

This paper is focused on the concept of simultaneous coating and texturing using a laser source. The use of laser for surface engineering offers great flexibility and presents manifold advantages [6]. By carefully modulating the laser optics and processing parameters it is possible to produce tailor made surfaces for various applications [7].

However, a major problem associated with engineered surfaces like coatings or textures for bio applications is their physical characterization. Generally, a surface is characterized by a large number of length scales mutually superimposed onto one another. The arithmetic average roughness, R_a , or the root mean square average, R_q (rms), commonly used to characterize the surface roughness do not convey information on the range of length scales over which different topographic features exist. The roughness measuring instruments often provide different values for surfaces at different scales depending on the resolution and the filtering capabilities of the instrument at that length scale. Therefore, surfaces should be characterized in a way such that the structural information at all scales is retained [8]. Over the last few decades researchers have tried to characterize multi-scaled surfaces using the mathematical concept of fractals which are invariant with respect to scale. Fractals are unique because of their extreme fragmentation bounded by non-euclidean geometry instead of topological dimensions. These fractals are quantified by fractal dimension, D_f , which permits to distinguish fractals at any scale.

Typically the calculation of fractal dimensions of engineering surfaces is a complicated process since it involves not only a number of mathematical models but also surface topography image processing. These fractal dimension calculators are built into commercial surface instruments, such as atomic force microscope (AFM) and Talysurf PG I [9]. Apart from being costly the fractal dimension calculators attached with these instruments cannot be used to calculate the surface fractal dimension of data acquired by other equipments. In light of this, the present paper reports a laser based technique to simultaneously coat and texture surfaces with potential for bio applications and deals with simple fractal based analysis to characterize surfaces for their multi-scale nature using a free public domain software called ImageJ (available with National Institutes of Health, USA).

2. Materials and methods

Ti alloy (Ti-6Al-4V) plates were cut into small coupons (25 mm × 25 mm × 3 mm) using Techcut10™ Allied High Tech Products Inc. The starting powders zir-

conia (ZrO_2) (stabilized with 5.4 wt% Y_2O_3) were obtained from Goodfellow Cambridge Limited, England. The mean particle size of zirconia powder used in this process was less than 1 μm . The coupons were sand blasted and rinsed with acetone. Using an air spray gun the zirconia powder mixed with a water based organic solvent was sprayed onto these coupons to achieve a uniform thickness of 40 μm .

In this work, a pulsed Nd:YAG laser (Trumpf Laser and VectorMark workstation) was employed. This laser emits infrared radiation of wavelength 1064 nm. With a focus diameter of 40 μm it is capable of delivering a fundamental-mode beam quality with pulse frequencies ranging from 1–60 kHz. In the present efforts, the samples were processed with 25 W power at frequency of 10 kHz for three different traverse speeds of 40 cm/min, 160 cm/min and 290 cm/min. For the purpose of covering the entire surface of the sample the overlapped laser pulses were laid in a linear track and such successive linear tracks were laid with a fixed overlap between them. The overlap between successive passes was 20% whereas the successive laser pulsing spots in a linear track resulted in an overlap of 95%, 80 and 70% for processing at 40 cm/min, 160 cm/min and 290 cm/min respectively.

Using Philips Norelco X-ray diffractometer the starting powders as well as the coatings were characterized with $\text{Cu K}\alpha$ radiation operated at 30 kV and 20 mA. The diffraction range was from 20° to 100° with a step increment of 0.02° and a count time of 1 s. Surface morphology was evaluated using a Hitachi-3500 scanning electron microscope (SEM) (Hitachi, Tokyo, Japan). The images were recorded at various magnifications and were further processed using conventional image processing techniques. Each of these images were converted from spatial domain of brightness to a frequency domain components using fourier transforms, filtered from noises and then thresholded to convert them into a binary digital image. A parameter called fractal dimension was calculated from these binary images by implementing a box counting technique using macros available in the public domain software ImageJ available with National Institutes of Health (NIH) USA.

Surface roughness of the coated samples was measured using a Mahr Federal profilometer. This is equipped with a stylus based tip which traverses the surface following the local irregularities. The motion of the stylus tip is recorded by a photoelectric cell and amplified. The stylus tip has a radius of 2 μm . In each measurement the tip traces a length of 5.6 mm and different roughness parameters like R_a (arithmetic mean deviation of the roughness profile), R_z (mean peak to valley height), R_{max} (maximum roughness depth) were recorded. Six different profiles were analyzed for each sample and the average value was reported.

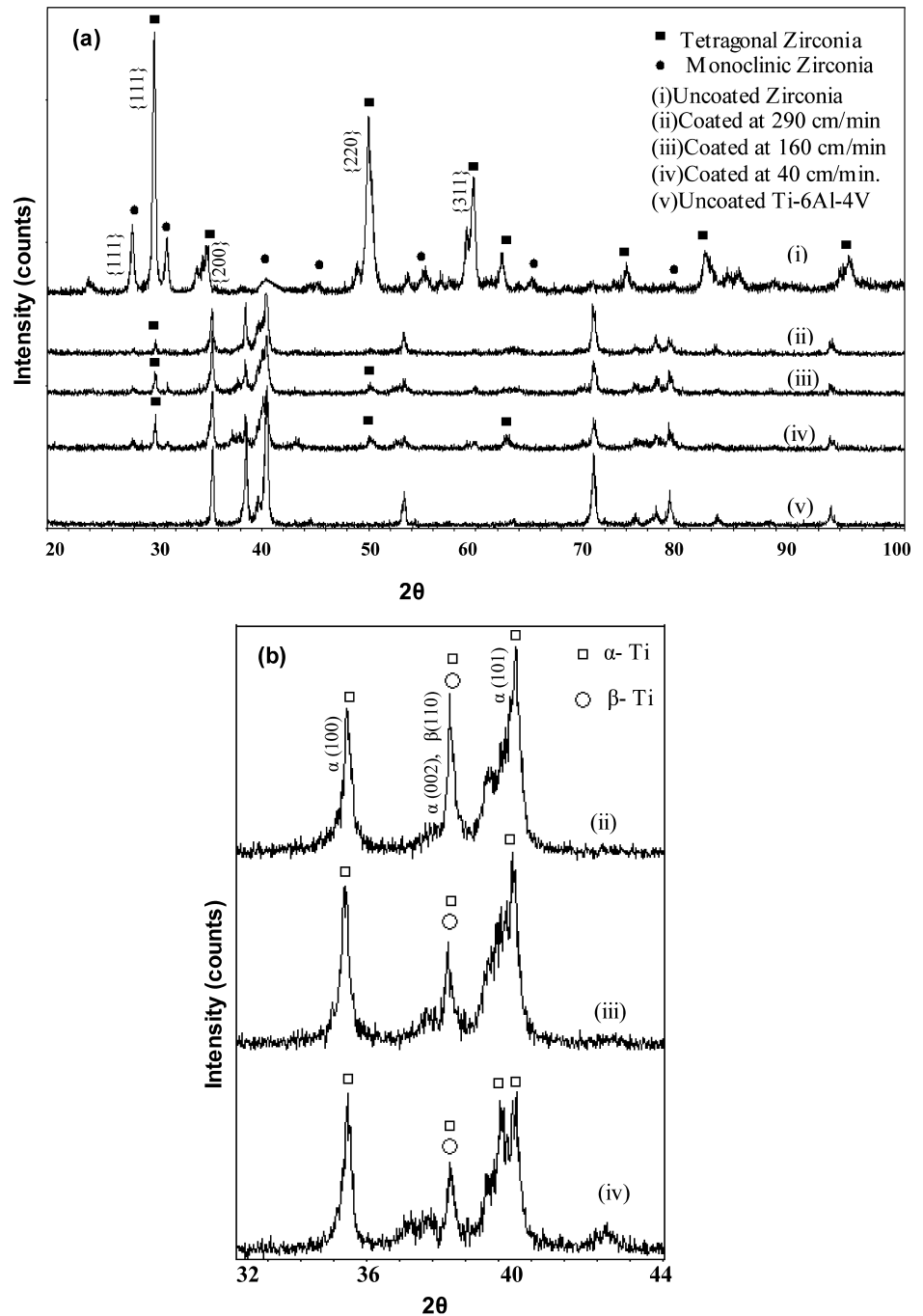
3. Results and discussions

3.1. Phase evolution in coating and substrate

Since laser processing is energy intensive operation variation in processing speed (at constant pulse frequency of 10 kHz) is expected to influence the total heat input and subsequently the phases evolved in the final material. X-ray diffraction (XRD) analysis was, therefore, carried out to evaluate the changes. Fig. 1a shows the overlaid XRD spectra of zirconia

powder, Ti-alloy (Ti-6Al-4V) substrate along with the coatings. The XRD analysis of zirconia powder indicated the existence of primitive tetragonal phases. Two small peaks at 28.1° and 30.6° indicated the presence of monoclinic phase in the powder. The coatings on Ti-6Al-4V showed the existence of zirconia peaks along with the substrate peaks. As the speed of the laser processing decreased the intensity of {111} peak corresponding to retained zirconia on the surface increased (Fig. 1a). The variation in the intensity of {111} peak can then be semi-quantitatively related to the variation

Fig. 1 XRD spectra for (a) Zirconia powder, and coatings produced at various speeds and (b) coatings scanned between 32°–44° for detailed phase identification.



in amount of retained zirconia. Furthermore, as expressed earlier, the total heat input (at constant pulse frequency of 10 kHz) is a function of processing speed and, therefore, a function of maximum temperature attained during the process [10, 11]. As the processing speed increases, the interaction time of laser beam with and subsequently the maximum temperature attained by substrate decrease. Thus the level of maximum temperature is expected to influence the characteristics of mixing and bonding between the coating precursor and the melted portion of substrate material [10, 12]. It is, therefore, in the present work the amount of retained zirconia in the laser modified region expected to decrease as the processing speed increased which may be the major cause for low intensities of zirconia peaks at higher processing speeds.

At the same time the variation in speed also offered possibilities for various Ti-alloy phase transformations within the laser modified surface region. A detailed observation of this was carried out by running new X-Ray scans from 32° – 44° where intense and major peaks of Ti exist (Fig. 1b). The speed of laser processing is expected to influence the rate of cooling cycle [10]. Accordingly, processing at 290 cm/min would set up extremely high thermal gradients compared to 40 cm/min. Under the condition of such high thermal gradient the kinetics of phase transformation is greatly influenced and can lead to various events such as but not limited to incomplete phase transformation and formation of unconventional phases [13–16]. Such changes are evident from the XRD spectra presented in Fig. 1a and 1b. In Ti-6Al-4V at high temperature ($>1100^\circ\text{C}$) β -Ti phase exists and during the cooling from these high temperatures the β -Ti tries to transform into α -Ti [17]. In the contrast, in the present work the amount of retained β -Ti seemed to have increased with processing speed suggesting that sufficient time was not available for it to transform into α -Ti. Using a direct comparison of the X-ray diffraction spectra the ratio of retained β -Ti to α -Ti were determined [18]. These values were plotted as a function of processing speed in Fig. 2. The retained β -Ti is harder, stronger and less ductile [17]. The alpha phase generally present in such a rapid quenching process is commonly referred to martensitic α [17]. The formation of this martensitic α is associated with distortion of the lattice resulting in a strained material. This α martensite is usually hard, tough and stronger and possesses better fatigue properties than α -Ti, which is relatively tough, soft and ductile [17]. Thus in the present experiments the distribution of martensitic α -Ti phase in β -Ti matrix (the ratio of retained β -Ti to α -Ti) is expected to result in a material that is hard and tough with improved mechanical properties compared to the untreated surface. This observation is in line with the observations made by the authors in their earlier work on Ti-alloys where laser induced microstructures seemed to have exhibited enhanced physical (tribological) and chemical (corrosion) properties in

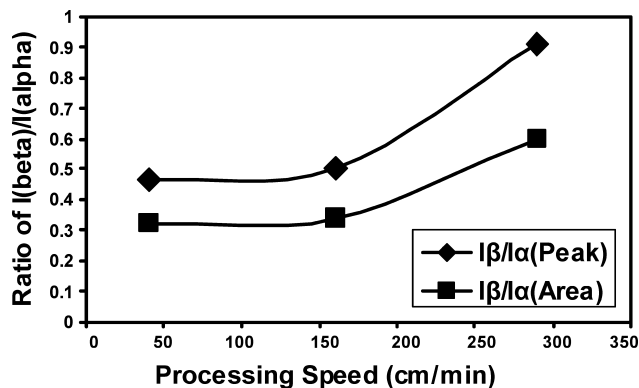


Fig. 2 Figure showing the ratio of retained β -Ti to α -Ti at various laser-processing speeds.

simulated bio-environment [19, 20]. Such manipulation for type and amount of phase within the coating for improved wear and corrosion properties is extremely important in tailoring the properties for bio applications such as hard tissue implants.

It appeared that for samples processed at 40 cm/min there were multiple sub peaks corresponding to $\{101\}$ class of reflections in the XRD spectrum (Fig. 1b). This could be the effect of cyclic thermal heating and cooling due to successive passes that in turn set up varying thermal gradients in previously melted tracks. Since β -Ti to α -Ti transformation is mono-variant in nature, the phases precipitated at different cooling rates are expected to have different morphologies which may result in different levels of residual stresses leading to the formation of α -Ti phases with different 'c' and the same 'a' lattice parameters [16]. On the contrary, when the laser processing speed increases sufficient time is not available for formation such different α -Ti phases which is evident from a few corresponding well defined multiple peaks in XRD spectra (Fig. 2b).

3.2. Morphological evaluation of textured coating

The chemical phase transformations induced during laser processing have been shown to influence the topographical modifications [21]. The following section deals with characterization of surface topography and its correlation with processing conditions. The surface morphology was influenced by the processing speed (at constant pulse frequency of 10 kHz) as can be seen from the scanning electron micrographs in Fig. 3. The processing speed influences the laser beam interaction time (total heat input) with the substrate and also the distance between the subsequent laser pulses (an overlap of 95%, 80 and 70% for processing at 40 cm/min, 160 cm/min and 290 cm/min respectively). These parameters together greatly influence the surface morphology. As seen in Fig. 3, each pulse produces a crater of solidified material with trough around the edge and relatively flat region inside

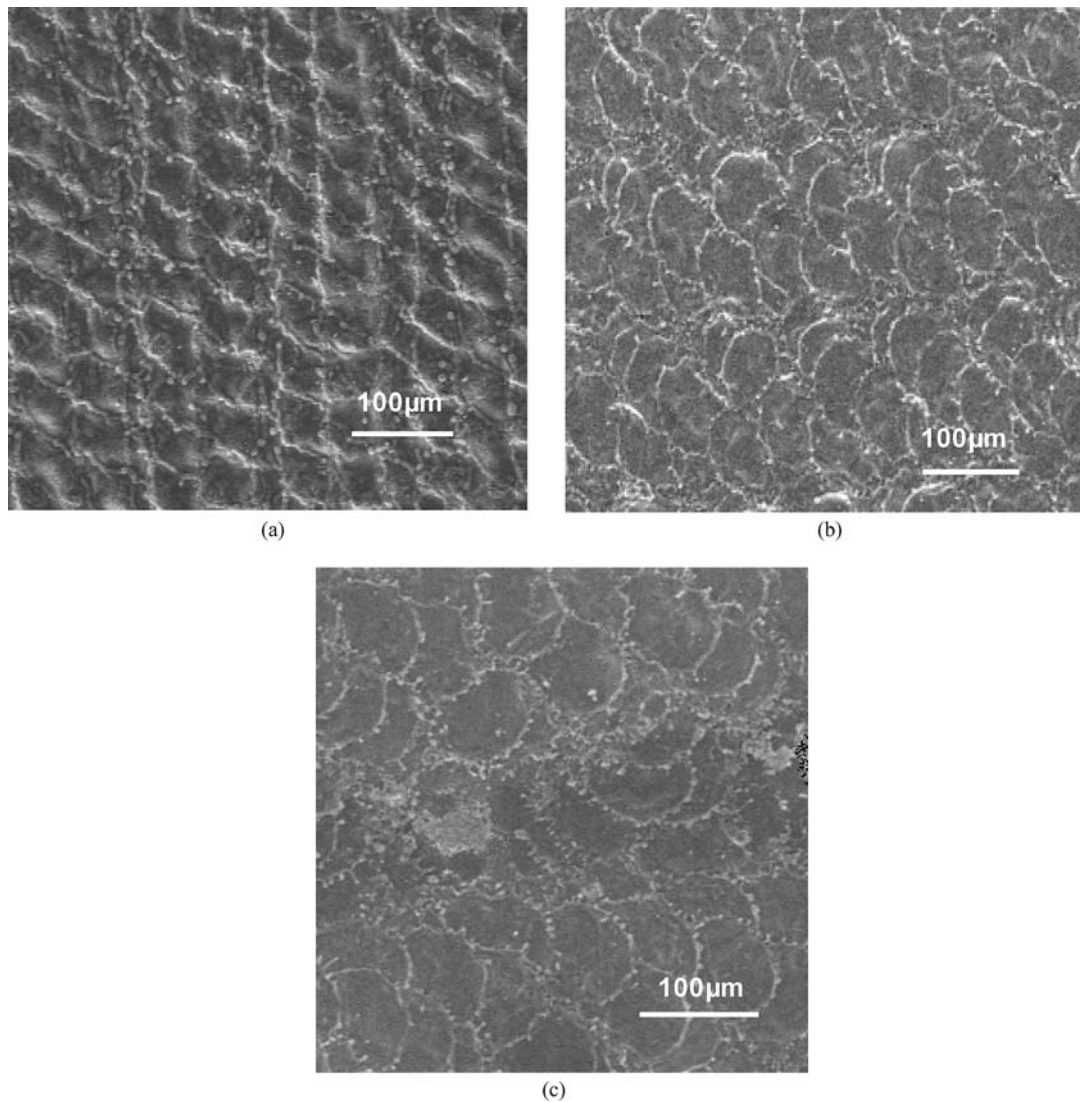


Fig. 3 Low magnification images of textured Ti-6Al-4V coupons processed at the speed of (a) 40 cm/min (b) 160 cm/min (c) 290 cm/min.

of the crater. The decrease in processing speed increases the overlap between subsequent pulses (craters), which further increases the trough region (Fig. 3a) and affects roughness of the processed surface region. However, repeated pulses in a linear track followed by several such linear tracks in overlapped manner (for coverage of the entire surface) change thermal gradients in the molten material which in turn can affect the nature and amount of trough and flat regions after solidification. Such situation can provide complex relationship between processing parameters and roughness of the surface.

Furthermore, the textures when closely observed at higher magnifications showed multi-scaled features. Fig. 4 included the image at higher magnification of the surface of sample processed at 40 cm/min that revealed a multi-scale texture. Similar observations were recorded for samples processed at other speeds (160 cm/min and 290 cm/min). The speed

of laser processing coupled with number of pulses per unit area seems to have influenced the outcome of the process. In order to interpret these features and quantitatively explain them, profilometer based roughness characterization was carried out. Although the profilometric measurements do not provide any idea about multi-scale nature of morphological features on the surface, they are very helpful in quantifying the roughness due to such features at a given single scale.

The variation in calculated roughness values for the three different speeds of operation is presented in Fig. 5. It can be observed that processing at 160 cm/min provides higher roughness parameters compared to the other conditions. The two processing parameters that influence the nature of the surface produced are the number of pulses per unit area and the repeated linear passes during the laser processing operation. The low roughness values for the sample processed at 40 cm/min can be explained based on the softening of the

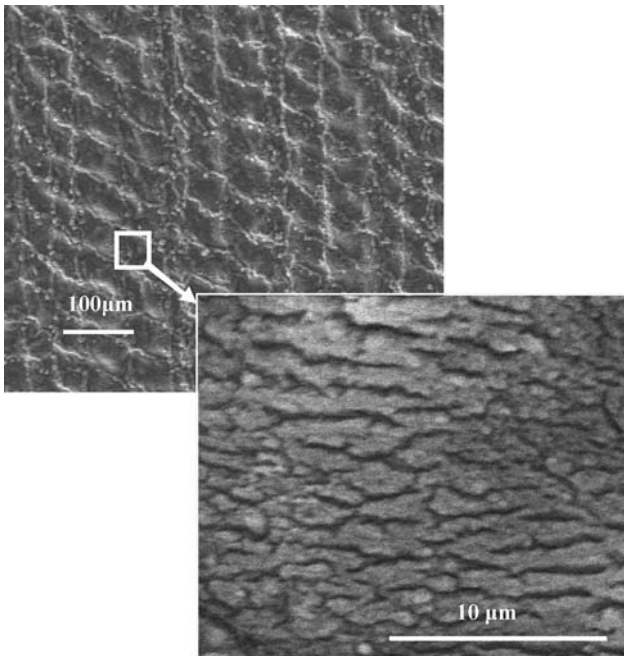


Fig. 4 Multi-scale features delineated with scanning electron microscopy observation for the sample processed at 40 cm/min.

peaks due to repeated passes of the laser source as shown in Fig. 6a. Apart from this the number of pulses per unit area increases as the speed of processing decreases due to which the temperature of the peaks is repeatedly maintained at higher level resulting in re-melting of the solidified peaks that lead to a smoothing effect on the surface. The smoothing effect decreases and roughness increases as the processing speed increases. However, at highest processing speed corresponding to 290 cm/min lower roughness can be attributed to the fact that the numbers of pulses per unit area are few and their degree of overlap is small due to which the topography consisted of alternate smooth and rough areas as presented in Fig. 6b.

As described in earlier sections the laser processing resulted in multi-scale structures (Fig. 4) and thus conven-

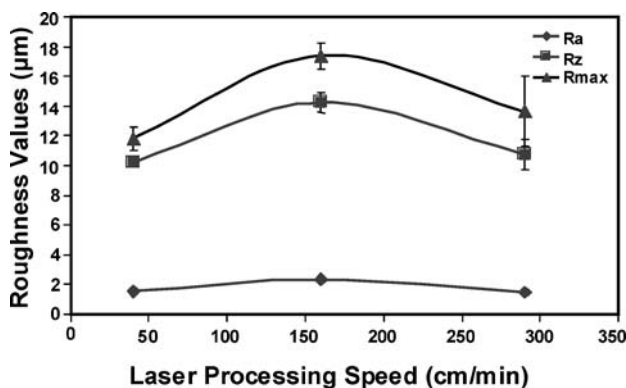


Fig. 5 Roughness parameter (with standard deviations) as function of laser processing speed.

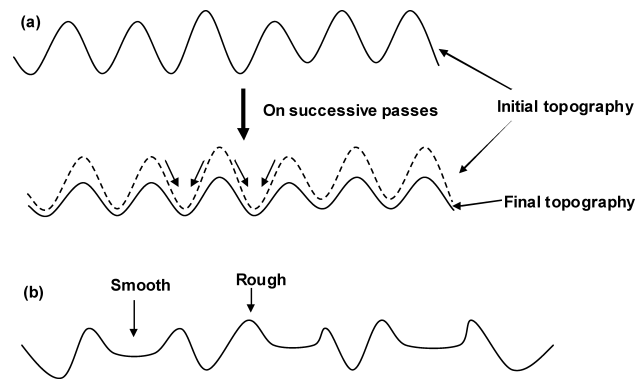


Fig. 6 (a) Schematic showing a possible smoothing effect at low processing speed of 40 cm/min. (b) Alternate smooth and rough surface produce due to past laser processing at 290 cm/min.

tional surface characterization parameters like Ra, Rz limit the range of observations to a single scale. In order to realize the multi-scale level of the features, a fractal-based approach was adopted. The fractal dimensions were determined from the SEM images processed using the macros based on the box counting technique in the software called ImageJ. The series of operations carried out to determine the fractal dimension is schematically shown in Fig. 7.

One of the most common methods for calculating the fractal dimension of a self-similar fractal is the box counting method. This process involves covering a structure with boxes of length ‘l’ and counting the number of boxes ‘N(l)’ required to cover the structure. The fractal dimension ‘D’ is given by

$$D = -\lim_{l \rightarrow 0} [\log_{10} N(l) / \log_{10} (l)]$$

where N(l) is number of boxes needed to completely cover the structure. D corresponds to the slope of the plot $\log_{10} N(l)$ versus $\log_{10} (l)$. The next most important parameter to be studied is the range of scales over which the micro features continue to show fractal nature. In order to predict this, the fractal dimensions were calculated from SEM images processed at different magnifications such as presented in Figs. 3 and 4. Since all the images were obtained under similar operating conditions and all had the same digital resolution the length per pixel was calculated for each magnification and this forms the basis for comparing the fractal dimensions at different magnifications as shown in Fig. 8. From this graph it can be concluded that all the three processing conditions show fractal properties at certain length scales. While processing at 40 cm/min resulted in structures that are fractal across a large number of length scales, faster processing conditions seems to have resulted in fractal nature over fewer length scales with fractality at two different length scales for the processing speed of 160 cm/min within the range of magnification employed for image observations/processing

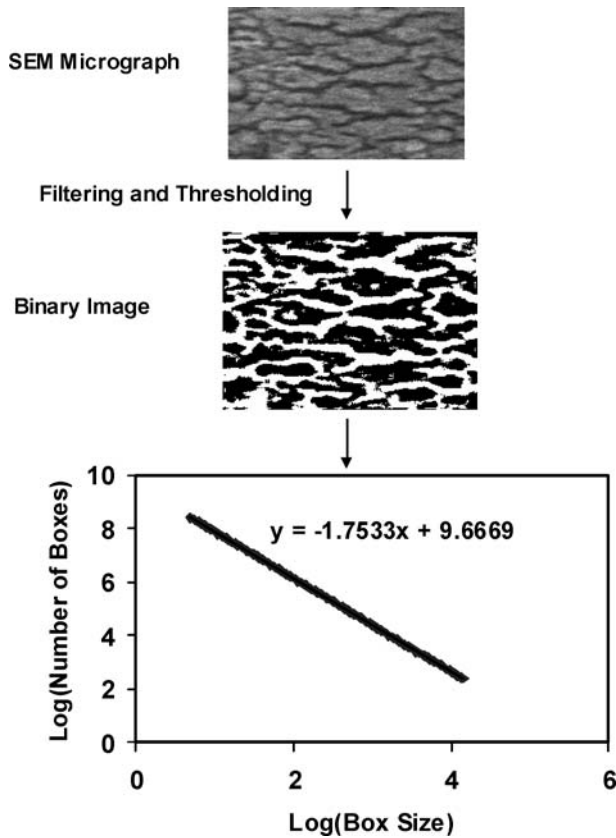


Fig. 7 Sequence of various image processing operations involved in fractal dimension determination. The slope of the log–log plot in the schematic shown corresponds to the fractal dimension (box counting technique).

in the present work. The upper limit of such magnification was $2 \mu\text{m}/\text{pixel}$ and it was dictated by the radius of the stylus tip ($2 \mu\text{m}$) on the profilometer used in roughness measurements.

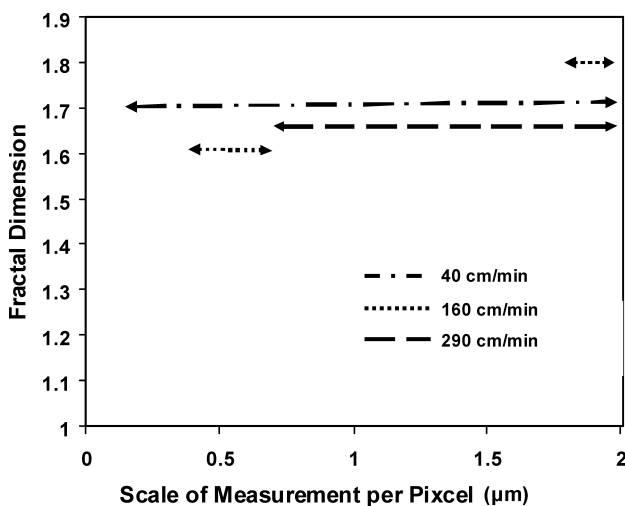


Fig. 8 Variation in fractal dimension at various length scales.

Table 1 Fractal dimension at different processing speeds

Speed of Laser Processing	Fractal Dimension at Length Scale of $2 \mu\text{m}$ Per Pixel
40 cm/min	1.7427
160 cm/min	1.8566
290 cm/min	1.6831

In light of the above findings, exploration of the relationship between fractal dimensions and roughness was considered important. Hence the fractal dimensions obtained at length scales of $2 \mu\text{m}$ (comparable to that of stylus tip dimension used in roughness measurements) are shown in Table 1. As can be seen, the variation in fractal dimensions is analogous to their roughness variation establishing the fact that fractal dimension can be correlated with general nature of roughness measurements and the fractal based predictions are reliable for different length scales. Although in the present case, such correlation was possible only at one length scale ($2 \mu\text{m}$), it is expected to follow appropriate trend at other length scales if and when roughness measurements are conducted at those scales. Roughness measurements at much finer length scales ($< 2 \mu\text{m}$) and determination of their relationship with fractal dimensions is the goal of future efforts. Such a fractal based description is useful in modeling the outcome laser processing to tailor multi-scaled structures at predetermined processing conditions.

The thickness of these laser induced coatings was about $40 \mu\text{m}$ and based on initial scratch testing these coatings appeared fairly adherent. However, the authors wish to determine the adhesive strength of coatings using a technique similar to that described by Nowotny *et al.*, who investigated the fused oxide ceramics on metallic substrates using a high power CO_2 laser [4]. In addition to evaluation of coating adhesion, the authors intend to evaluate the response of coating in bio-environment for protein, cell, and tissue integration along with corrosion response. These results will be presented in due course of time. Since the physical structure of a biomaterial is now considered a key factor in determining cellular responses and further adhesion and integration into bioenvironment, laser based processing can be experimented with to tailor organized structures for direct biomedical applications

4. Conclusions

In the present work it has been successfully shown that lasers can be used to coat and texture simultaneously to produce surfaces that are hierarchically integrated and organized at multiple scales. The amount of ziconia retained as coating and the kinetics of phase transformations within the matrix of

coating area are influenced by the speed of laser processing. The retained β -Ti phase increased and retained Zirconia decreased with the speed of processing. The number of pulses and successive laser passes seemed to influence the roughness of the final surface. A fractal-based approach was used to interpret the multi-scaled surfaces and has been successfully correlated with the surface roughness values. Processing at 40 cm/min resulted in coating rich in zirconia and surface being fractal over wider range of length scales compared to other processing speeds.

Acknowledgments The authors acknowledge the assistance from Fred Schwartz and Doug Warnberg of the Center for Laser Applications at the University of Tennessee Space Institute in laser processing the samples.

References

1. G. HASAN and Ç. HÜSEYİN, *Biomaterials* **25** (2004) 3325.
2. H. GULERYUZ and H. CIMENOGLU, *Surf. Coat. Technol.* **192** (2005) 164.
3. Y. YANG, J. L. ONG and J. TIAN, *Biomaterials* **24** (2003) 619.
4. S. NOWOTNY, A. RICHTER and K. TANGERMANN, *J. Thermal Spray Technol.* **8** (1999) 258
5. J. TAN and W. M. SALTZMAN, *Biomaterials* **25** (2004) 3593.
6. A. KURELLA A and N. B. DAHOTRE, *J. Biomat. Appli.* (2005) Accepted.
7. A. C. DUNCAN, F. WEISBUCH, F. ROUAIS, S. LAZARE and CH. BAQUEY, *Biosensors and Bioelectronics* **1** (2002) 413.
8. P. F CHAUVY, C. MADORE C and G. LANDOLT, *Surf. Coat. Technol.* **110** (1998) 48.
9. C. Q. YUAN, J. LI, X. P. YAN and Z. PENG, *Wear* **255** (2003) 315–326
10. P. KADOLKAR, H. WANG, T. R. WATKINS and N. B. DAHOTRE, *International J. of Adv. Manuf. Technol* **23** (2003) 350.
11. S. NAYAK, H. WANG, and N. B. DAHOTRE, *Materi. Sci. Technol.* **20** (2004) 1609.
12. N. B. DAHOTRE, P. KADOLKAR and S. SHAH, *Surf. Interface Analysis* **31** (2001) 659.
13. A. SINGH and N. B. DAHOTRE, *Metall. Mater. Transact. A* **36** (2005) 1.
14. A. AGARWAL and N. B. DAHOTRE, *Metall. Mater. Transact. A* **31** (2000) 401.
15. L. R. KATEPELLI, A. AGARWAL and N. B. DAHOTRE, *Appl. Surf. Sci.* **153** (1999) 65.
16. S. MALINOV, W. SHA, Z. GUO, C. C. TANG and A. E. LONG, *Materials Characterization*, **48** (2002) 279.
17. S. ABKOWITZ, J. J. BURKE and R. H. HILTZ JR., in “Titanium in Industry” (D. Van Nostrand Company, Inc. New York, 1955) p. 50.
18. B. D. CULLITY, in “Elements of X-Ray diffraction” (Addison-Wesley Publishing Company, Inc. Philippines, 1978) p. 397.
19. R. SINGH, M. MARTIN and N. B. DAHOTRE, *Surface Engineering*, (2005), Accepted for publication.
20. R. SINGH, A. KURELLA and N. B. DAHOTRE, *J. Biomat. App.*, (2005), Accepted for publication.
21. F. GUILLEMOT, F. PRIMA, V. N. TOKAREV, C. BELIN, M. C. PORTE-DURRIEU I, T. GLORIAN, CH. BAQUEY and S. LAZARE, *Appl. Phys. A* **77** (2003) 899.